MILITARY TECHNICAL COLLEGE
CAIRO - EGYPT

7th INTERNATIONAL CONF. ON
AEROSPACE SCIENCES &
AVIATION TECHNOLOGY

IMPROVED COMPACT SIGNATURE ANALYZER BASED ON MULTIPLE INPUT SHIFT REGISTER (MISR)

M. S. GhONIEMY* **REDA H. SEIREG**** **SAYED F. BAHGAT****

AHMED S. MOHAMED***

Abstract :

The Multiple Input Compact Signature Analysis (MICSA) has been proposed to reduce the hardware of compaction technique by 50 %. The general formula for the corresponding Aliasing Error Probability (AEP) has been found to lie between 0 and 1, depending on the CUT, and the construction of the MICSA. The hardware conditions for the SS-AEP to be equal to 2^{-k} is obtained, leading to the Improved Multiple Input Compact Signature Analyzer (IMICSA). The theoretical analysis and simulation results indicated that for the MICSA, if its k^{th} stage is not connected to any of the CUT's inputs, then, The SS-AEP is equal to the reciprocal of 2^k, where k is the number of the stages of the signature analyzer, regardless of the construction of CUT, or the initial state of SA. This result indicates that for the IMICSA the more stages are there in MISR the better is the SS-AEP.

---

* Professor, Faculty of Computer Science & Information Systems, Ain Shams University.
** Associate Professor, Military Technical College, Cairo, Egypt.
*** Teacher, Military Technical College, Cairo, Egypt.

1. Introduction :

In digital circuits, testing is achieved by applying a sequence of input stimuli, known as *test vectors*, generated by Test Pattern Generator (TPG) and checking for possible faults in the circuit by producing observable faulty response at primary output called "Signature", generated by a Data Compressor (DC). This signature is then compared against a known one (REF), where a judgment can be made about the correctness of the circuit [3], [4],[5], [9], [10],[12], [13], [14], [15], [17].

The signature algorithm should not lose information. Specifically it must not lose the evidence of a fault indicated by a wrong response from CUT. This is refers to *Masking* (Aliasing Error Probability AEP) effect which is the compression of an erroneous output sequence from a faulty circuit into the same signature as the fault free circuit[2], [7], [11], .

Multiple Input Shift Registers (MISR) is a preferred technique used to realize efficient built-in self-test (BIST) of digital VLSI circuits, it is used extensively as a source for pseudo random binary test sequences and as a means to carry out response compression - known as *signature analysis* [8], .

This leads to the idea of multiple input compact signature analyzer (MICSA)[18],[19], in which one unit, constructed from MISR, connected in a closed loop form with the CUT, is used as a random test pattern generator and signature analyzer at the same time, as shown in Fig. 1, to reduce the hardware of signature analysis compaction technique by 50 %.

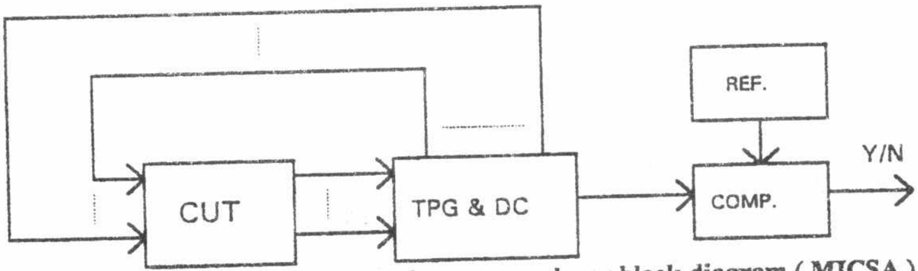

Fig. 1 Multiple inputs compact signature analyzer block diagram (MICSA).

The following sections introduce a deep analytical study of the SS-AEP of MICSA and how it depends on each of the following factors :

1- The structure of the CUT.
2- The probability of faulty & non-faulty CUT.
3- The number of signature analyzer stages k.
4- The type of the polynomial used in realizing the MISR (primitive or non-primitive).
5- The particular way by which the MISR is implemented.
6- The location of points of connection of the MISR outputs with the CUT inputs.

2. SS-AEP For Multiple Input Compact Signature Analyzer :

To study the steady state performance of MICSA, we modeled the proposed system using Markov process [1], moreover the SS-AEP is calculated.

To calculate the SS-AEP for the MICSA using Markov process, several mathematical manipulations are used :
1- Modeling the MICSA circuit connected with CUT by generating the Markov State Diagram (MSD).
2- Constructing the Transition Probability Matrix (TPM),then Multiplying it by itself n times, where n tends to infinity.
3- Deducing and solving the local balance equations of the system [1].
4- Plotting the solved local balance equations, to analyze their behavior.

The general construction of multiple input compact signature analyzer is shown in Fig. 2, where G(x) represents a net of XORs used to implement of the MISR, and $f(X_1), f(X_2),........,f(X_k)$ represent the outputs of the CUT.

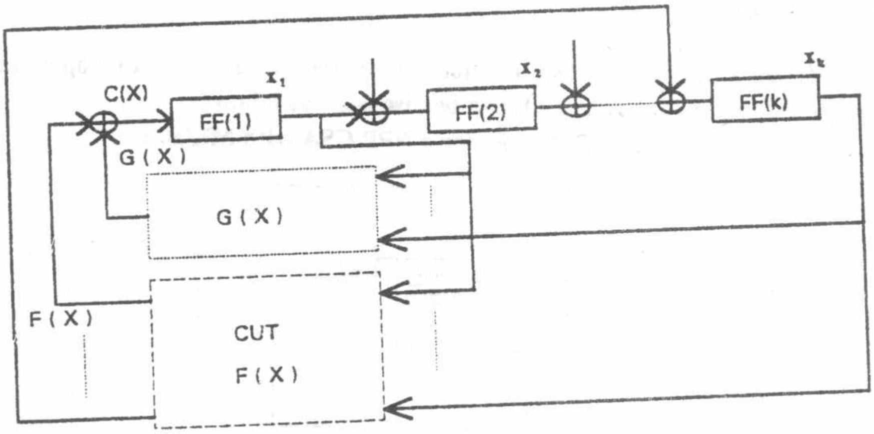

Fig. 2 The general construction of multiple input compact signature analyzer .

As shown in Fig. 2, the MICSA, has two XORed loops (functions). The first loop; denoted as the main loop; comprises the shift register stages and the feedback lines as inputs to G (X).

$$G(x) = \sum_{m=1}^{k} a_m x_m \tag{1}$$

where $a_1,........,a_k$ have the values zero or one, and the summation is modulo-2 adder.

then :

$$G(x_m) = g(x_1, x_2,.......,x_k) \tag{2}$$

The second loop; denoted as the CUT-loop, contains the shift register stages and the CUT, having the function $f(x_1, x_2,.......,x_n)$.

The XORing of these two functions is C(X), where :

$$C(X) = g(x_1, x_2,......,x_m) \oplus f(x_1, x_2,.......,x_n) \tag{3}$$

where $m = 1,......, k$ & $n = 1,......, k$

Since we use MISR, where all states are reachable from each other, the system can be modeled by irreducible Markov chain [1]. If a Markov chain is irreducible, recurrent nonnull, and aperiodic (i.e., it is ergodic), there exists a unique limiting distribution for the probability of being in a state S_i denoted as π_{S_i} independent of the initial state. These probabilities are called steady-state or equilibrium probabilities.

If the system can be represented by a doubly stochastic matrix, then the probability of existing at any state is equal to the reciprocal value for the number of these states. Therefore, the AEP is equal to the probability of existing at any state.

Theorem :

For the CSA which is constructed from MISR, if its k th stage is not connected to any of the CUT's inputs, then, The SS-AEP is equal to the reciprocal of 2^k , where k is the number of the stages of the signature analyzer, regardless of the construction of CUT, or the initial state of SA.

Proof :

This proof is divided into two sections :

1) Proving that if the k^{th} stage of MISR is connected to any of the CUT's inputs, then the behavior of the CSA using MISR depends on the structure of CUT and it will lose its linearity. Otherwise, it will keep the MISR characteristic.

2) Proving the validity of the theorem.

1- The different cases of the XOR of the two functions generated from the main loop and the CUT-loop $C(X) = g(x_1, x_2, \ldots\ldots, x_m) \oplus f(x_1, x_2, \ldots\ldots, x_n)$, can be discussed as follows :

A) When connecting the last stage to the CUT-loop, for a NPP CSA with MISR :

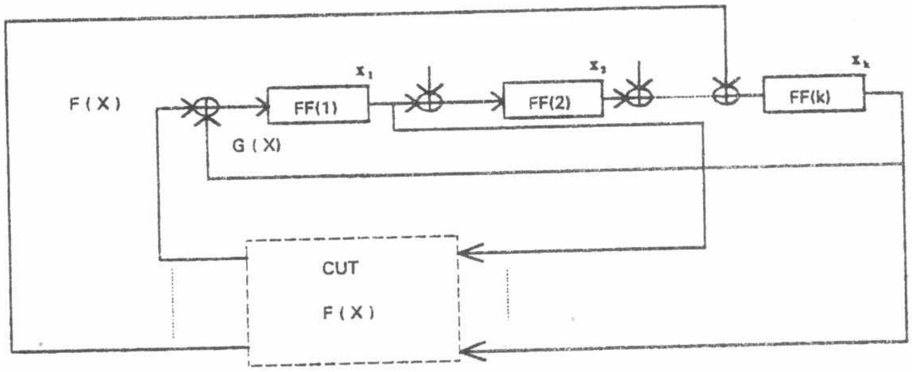

Fig. 3 Function diagram for MICSA with MISR, NPP, and connecting the last stage to CUT-loop.

From Fig. 3 $G(X) = g(X_k) = X_k$

$F(X) = f(X_1, X_2, \ldots, X_k)$

The XOR of these two functions is :

$$C(X) = f(x_1, x_2, \ldots, x_k) \oplus x_k = c(x_1, x_2, \ldots\ldots, x_{k-1}).$$

The above result shows that C (X) is independent of the last stage X_k. In other words, the MISR is independent of the feedback from X_k, which means that the main loop for MISR is open and the system depends only on the CUT-loop. However, The CUT in general is nonlinear, therefore, the system will become nonlinear too, except for the special case when the CUT is linear.

B) When connecting the last stage to the CUT-loop, for a PP CSA with MISR :

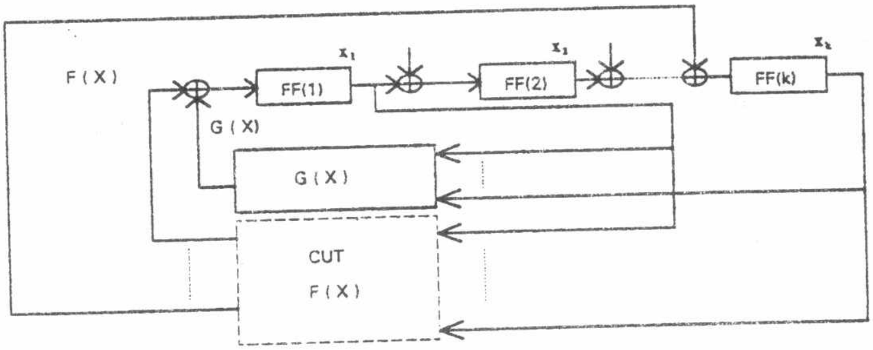

Fig. 4 Function diagram for MICSA with MISR, PP, and connecting the last stage to CUT.

From Fig. 4 $G(X) = g(x_1, x_2, \ldots, x_m)$

$F(X) = f(x_1, x_2, \ldots, x_n)$

- For the case when $m \neq n$ and the k^{th} stage is connected in both of the main loop and CUT-loop :

The XOR is reducing the outputs of the feedback shift register which agree with the CUT inputs Boolean function, and because that last stage is one of them (in this case), then its effect is reduced. That is to say, the

output of the XOR is independent of the feedback x_n, then some part of the circuit which include $(x_1, x_2, \ldots\ldots, x_{n-1})$ is linear, and the other parts are open (or not connected) to the MISR, but connected to the CUT, which in general is nonlinear, therefore, the system will become nonlinear, except for the special case when the CUT is linear.

- For the case when m = n = k and the k th stage is connected in both the main loop and CUT-loop :

If the number of feedback lines for G (X) (including the last stage) is equal to the number of inputs for the CUT, then the XOR of these two functions is :

$$C(X) = f(x_1, x_2, \ldots, x_k) \oplus g(x_1, x_2, \ldots, x_k) = C(0)$$

the output is equal to zero and does not depend on either MISR or CUT.

C) When the last stage is not connected to the CUT-loop, for a NPP CSA with MISR :

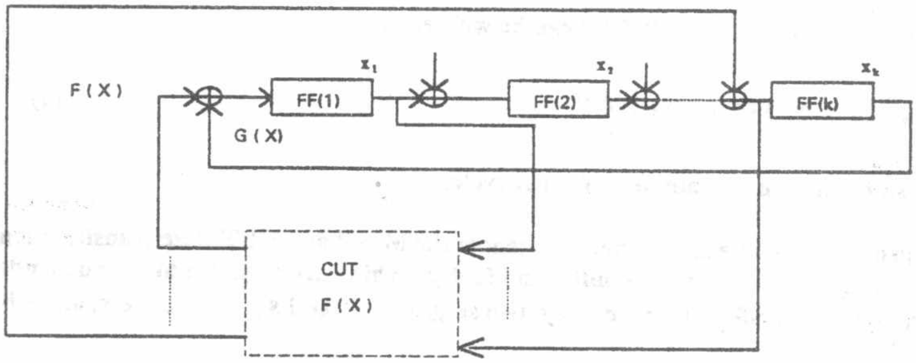

Fig. 5 Function diagram for MICSA with MISR, NPP, and not connecting the last stage to CUT.

From Fig. 5 $\quad G(X) = g(x_k) = x_k$

$$F(X) = f(x_1, x_2, \ldots\ldots, x_n)$$

then $\quad C(X) = f(x_1, x_2, \ldots, x_n) \oplus x_k = c(x_1, x_2, \ldots, x_n, x_k)$

Then the main loop is always closed, in other words, the MISR keeps its characteristics as a LFSR, so the system will be linear.

D) When the last stage is not connected to the CUT-loop, for a PP CSA with MISR :

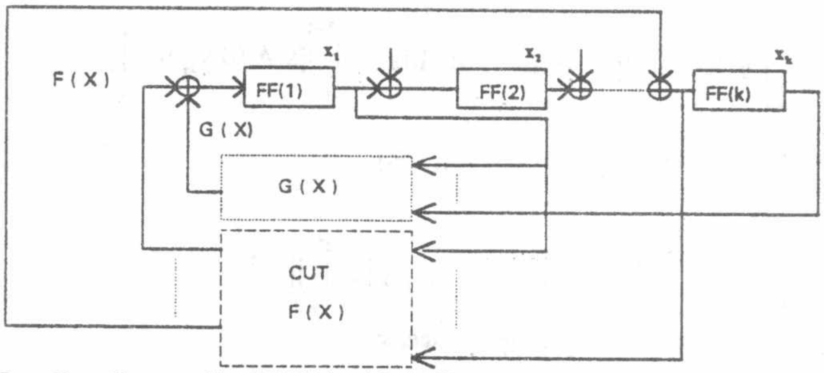

Fig. 6 Function diagram for MICSA with MISR, PP, and not connecting the last stage to CUT.

From Fig. 6 $\quad G(X) = g(x_1, x_2, \ldots, x_k)$

$F(X) = f(x_1, x_2, \ldots\ldots, x_n)$ **where k > n**

then $C(X) = f(x_1, x_2, \ldots, x_n) \oplus g(x_1, x_2, \ldots, x_{k-1}, x_k) = c(x_1, x_2, \ldots, x_{k-1}, x_k)$

- For the case when $k \neq n$ and the k^{th} stage is not connected in CUT-loop:

The XOR is reducing the outputs of the feedback shift register which agree with the CUT inputs Boolean function, and because the last k-stage is not one of them (in this case), then its effect is not reduced, then the XOR is a function of the outputs of the feedback shift register that does not agree with the CUT inputs Boolean function and the last stage x_k.

- For the case if all the CUT inputs Boolean function agree with n-1 outputs of the feedback shift register , and the k^{th} stage is not connected in CUT-loop:

then $$C(X) = f(x_1, x_2, \ldots, x_n) \oplus g(x_1, x_2, \ldots, x_n, x_k) = c(x_k)$$

Then the main loop is always closed , but the PP-LFSR in this case will depend only on x_k which makes it as NPP-LFSR.

2- The test process transition matrix (TPM) P can be written as :

$$P_{ij} = \text{prob}\left[S(n+1) = S_j \middle| S(n) = S_i\right] \tag{4}$$

with S denoting the MISR state, and n the number of clock cycle.

To prove that the process is double stochastic, let's denote the MISR and CUT state transition matrix by A, the error probabilities in shifting the sequence non-faulty and faulty - which are assumed to be independent - by X, Y, Z, and W respectively, and the MISR states with only two stages by s_{p_1} and s_{p_2} respectively, and with both set by s_{p_3} we get :

$$\left.\begin{array}{l} \text{prob}[s(n+1) = s_j | s(n) = s_i] = Y \quad \text{prob}[s_j = s_i A \oplus s_{p_1}] \quad + \\ Z \quad \text{prob}[s_j = s_i A \oplus s_{p_2}] + W \quad \text{prob}[s_j = s_i A \oplus s_{p_3}] + X \quad \text{prob}[s_j = s_i A] \end{array}\right\} \tag{5}$$

X being the probability of fault free operation.
Now since the events
$\left[S(n) = S_i, \left[i = 0 : 2^k - 1\right]\right]$ **are disjoint at any instant (n) then,**

$$\sum_{i=0}^{2^k-1} \text{prob}\left[S_j = S_i\right] = \text{prob}\left[S_j \in \bigcup_{i=0}^{2^k-1} [S_i]\right] \tag{6}$$

Hence

$$\left.\begin{array}{l} \sum_{i=0}^{2^k-1} P_{ij} = Y \quad \text{prob}[s_j \in \bigcup_{i=0}^{2^k-1} [s_i A \oplus s_{p_1}]] \quad + Z \quad \text{prob}[s_j \in \bigcup_{i=0}^{2^k-1} [s_i A \oplus s_{p_2}]] + \\ W \quad \text{prob}[s_j \in \bigcup_{i=0}^{2^k-1} [s_i A \oplus s_{p_3}]] + X \quad \text{prob}[s_j \in \bigcup_{i=0}^{2^k-1} [s_i A] \end{array}\right\} \tag{7}$$

But for MISR we know that :

$$\bigcup_{i=0}^{2^k-1}\left[s_i A \oplus s_{p_1}\right] = \bigcup_{i=0}^{2^k-1}\left[s_i A \oplus s_{p_2}\right] = \bigcup_{i=0}^{2^k-1}\left[s_i A \oplus s_{p_3}\right] = \bigcup_{i=0}^{2^k-1}\left[s_i A\right] = \bigcup_{i=0}^{2^k-1}\left[s_i\right] \tag{8}$$

Since each one of them covers the whole binary k tuple space, so

$$\text{prob}\left[S_j \in \bigcup_{i=0}^{2^k-1} [S_i]\right] = 1 \tag{9}$$

as S_j belongs to the same k- tuple binary space spanned by the union. Moreover, by definition the probability space of any error bit can be expressed as :

$$X+Y+Z+W=1 \tag{10}$$

since they cover the probability space of any error bit, then from (7), and (10) :

$$\sum_{i=0}^{2^k-1} P_{ij} = 1$$

Hence, the process is a double stochastic Markov process [1] (the TPM of a doubly stochastic Markov process has the property that each column and each row sum to one). Hence each state has an equal opportunity of appearing in the steady state, consequently;

$$\pi_{SS} = \frac{1}{2^k}(1,1,1......,1)$$

Where π_{SS} denotes the steady-state probability vector.

That is to say each state has an equal probability of occurrence at steady state regardless of the initial state. In particular

$$\text{prob}[S = S_0]_{ss} = 2^{-k}$$

where $S_0 = (0,0,.....,0)$

The AEP of the system is, in general, given by the probability of returning to the zero state, when starting from zero state, given that the system was not stuck-at this zero state. Note that the formulas derived above are valid for the zero initial state, and did not presume that the system was stacking-at zero. Consequently ,

$$\text{AEP}_{ss} = \text{prob}[S = S_0]_{ss} = 2^{-k} \tag{11}$$

Equation (11) reveals that the SS-AEP is a function of (k), and that the more stages in MISR the better the SS-AEP. Moreover, SS-AEP is shown to be independent of the type of the polynomial used in realizing the MISR, primitive or not, and independent of the particular choice of the Galois field polynomial used (within the same k). Furthermore, it is independent of the particular way by which MISR is implemented. It is also independent of the location of the input stage, independent of the initial state, and finally it is independent of the probabilities X, Y, Z, and W. Moreover, this proof can be extended to cover MISR with k inputs, and the value of SS-AEP rather than the previous proof for two input MISR.

Q.E.D.

3. Cases Studied for Multiple Input CSA (MICSA) :

For discussing the SS-AEP of the MICSA, the following cases are considered :

1- Structures for MICSA with the k outputs of the signature analyzer equal to the m inputs of CUT.
2- Structure for MICSA with k > m, and with Connecting Last Stage (CLS) of signature analyzer output (the k^{th} stage) to any of the inputs of CUT.

Then the structures for IMICSA (k > m, and with Not Connecting Last Stage (NCLS) of signature analyzer output (the k^{th} stage) to any of the inputs of CUT) for both PP-MISR and NPP-MISR will be studied.

This part studies the cases in which the number of outputs from the CUT are two. The error probability in shifting the sequence non faulty and faulty for the first output(O1) - which are assumed to be independent - is given by p, 1-p. The error probability in shifting the sequence non faulty and faulty for second output (O2) - which are assumed to be independent - is given by q, 1-q.

The following Table 1 includes the different cases for O1, O2 being faulty or non faulty.

Output (O1)	Output (O1)	Error probability	Symbol
Non faulty	Non faulty	p.q	X
Faulty	Non faulty	(1-p).q	Y
Non faulty	Faulty	p.(1-q)	Z
Faulty	Faulty	(1-p).(1-q)	W

Table 1 The different cases for O1, O2 being faulty or non faulty .

3.1 Structure of MICSA, k = m = 2, Outputs (O) = 2, CUT(1) :

Fig. 7 is composed of 2-stages (k) PP-MISR, the CUT(1) has two inputs and two outputs. The outputs of the 2-stage MISR are connected to the 2 inputs of the CUT (1) , while the outputs of the CUT(1) are fedback to the first and second stages of MISR through XOR circuits. Fig. 8 represents the MSD for Fig. 7, and its TPM is shown in Fig. 9.

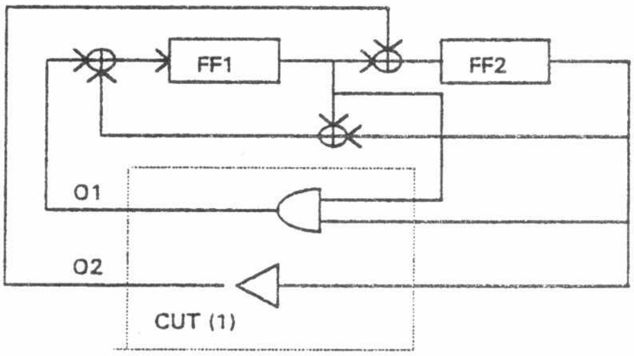

Fig. 7 Structure for MICSA, ith k = m =2, O = 2, CUT(1).

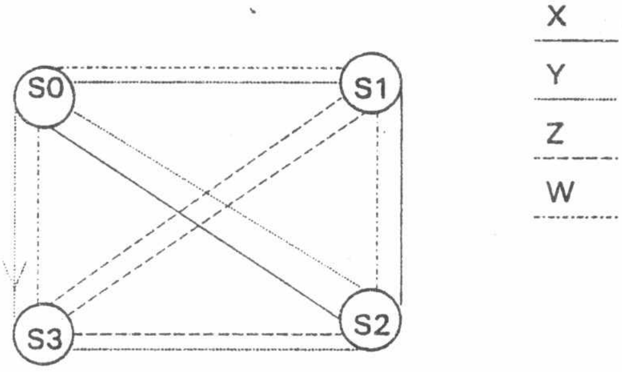

Fig. 8 MSD for MICSA, with k = m = 2, O = 2, CUT(1).

$$M1 = \begin{array}{c|cccc} & s_0 & s_1 & s_2 & s_3 \\ s_0 & Z & W & X & Y \\ s_1 & Y & X & W & Z \\ s_2 & Y & X & W & Z \\ s_3 & W & Z & Y & X \end{array}$$

Fig. 9 TPM for MICSA, with k = m = 2, O = 2, CUT(1).

From Fig. 9 the local balance equations are calculated as :

$$\begin{aligned} (1-Z)s_0 &= Ys_1 + Ys_2 + Ws_3 \\ (1-X)s_1 &= Ws_0 + Xs_2 + Zs_3 \\ (1-W)s_2 &= Xs_0 + Ws_1 + Ys_3 \\ s_0 + s_1 + s_2 + s_3 &= 1 \end{aligned} \qquad (12)$$

The equations (12) are solved using [16]; giving :

$$\left.\begin{aligned} s_0 &= \frac{(-YZ - Y^2 - W + XW + W^2)}{(-1 + X - XZ - ZW - Y + Z^2 + YW + XY - Y^2)} \\ s_1 &= \frac{-(XY - 2XYZ + Z - Z^2 - ZW + Z^2W + WY^2 + W^2 - W^3 + WX^2)}{(-1 + X - XZ - ZW - Y + Z^2 + YW + XY - Y^2)} \\ s_2 &= \frac{(-Y + YZ + XY - 2XYZ - ZW + Z^2W + WY^2 - W^3 - WX + WX^2)}{(-1 + X - XZ - ZW - Y + Z^2 + YW + XY - Y^2)} \\ s_3 &= \frac{(-1 + Z + W - ZW + X - XZ + YW + XY)}{(-1 + X - XZ - ZW - Y + Z^2 + YW + XY - Y^2)} \end{aligned}\right\} \qquad (13)$$

Substituting the values of X, Y, Z, and W in equation (13) by the corresponding values of p, q as described in Table (1), and simplifying the results, we get :

$$s_0 = \frac{(1-p)(-q-p+2pq)}{(-1+2pq-p-4p^2q-2q^2+4q^2p+2p^2)} \qquad (14)$$

$$s_1 = \frac{(-q+4p^2q^2+4pq-p-4p^2q+q^2+-4q^2p+p^2)}{(-1+2pq-p-4p^2q-2q^2+4q^2p+2p^2)} \qquad (15)$$

$$s_2 = \frac{(1-p)(-1+2q-4pq+p-2q^2+4q^2p)}{(-1+2pq-p-4p^2q-2q^2+4q^2p+2p^2)} \qquad (16)$$

$$s_3 = \frac{(-p+pq+p^2-2p^2q+2q^2p-q^2)}{(-1+2pq-p-4p^2q-2q^2+4q^2p+2p^2)} \qquad (17)$$

Equations (14 - 17) are plotted in Figures (10 - 13), each figure is followed by a matrix giving the values of the state probability against the error probability p and q.

These figures show that the state probability is depending on the error probability of the CUT(1), the threshold value (1/4) which is the SS-AEP of MISR in the open loop is greater or less than the probability of the corresponding CSA with MISR in closed loop system, but they are equal for the equally likely error model when p = q = 0.5, which is the same as the one given by [6].

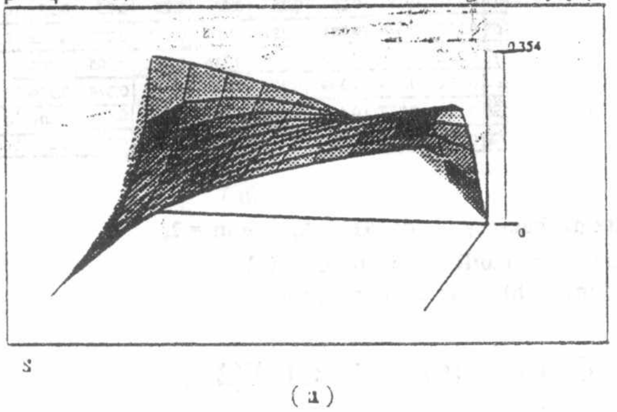

(a)

		0	1	2	3	4	5	6	7	8
	0	0	0.098	0.185	0.254	0.303	0.333	0.349	0.354	0.351
	1	0.083	0.15	0.21	0.26	0.297	0.321	0.335	0.339	0.337
	2	0.143	0.188	0.229	0.263	0.289	0.308	0.318	0.322	0.321
	3	0.187	0.216	0.241	0.262	0.28	0.292	0.299	0.302	0.301
	4	0.222	0.236	0.248	0.258	0.267	0.273	0.277	0.278	0.278
S =	5	0.25	0.25	0.25	0.25	0.25	0.25	0.25	0.25	0.25
	6	0.273	0.258	0.246	0.236	0.228	0.222	0.218	0.216	0.216
	7	0.292	0.258	0.233	0.213	0.199	0.188	0.18	0.175	0.174
	8	0.308	0.245	0.205	0.177	0.157	0.143	0.133	0.126	0.123
	9	0.321	0.201	0.147	0.116	0.097	0.083	0.074	0.067	0.064
	10	0	0	0	0	0	0	0	0	0

(b)

Fig. 10 Dependence of the state probability s_0 of MICSA, k = m = 2, and O = 2, upon the error probabilities of the CUT(1).
(a) Graphic representation. (b) Matrix representation.

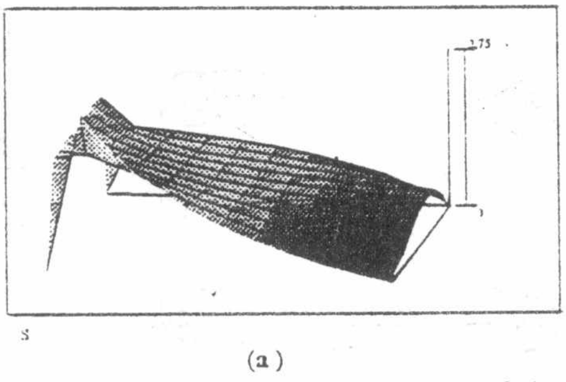

(a)

		0	1	2	3	4	5	6	7	8
	0	0	0.088	0.148	0.178	0.182	0.167	0.14	0.106	0.07
	1	0.083	0.137	0.173	0.191	0.192	0.179	0.156	0.128	0.097
	2	0.143	0.174	0.194	0.204	0.203	0.192	0.175	0.153	0.128
	3	0.187	0.203	0.213	0.218	0.216	0.208	0.197	0.181	0.164
	4	0.222	0.228	0.232	0.233	0.231	0.227	0.221	0.213	0.204
S =	5	0.25	0.25	0.25	0.25	0.25	0.25	0.25	0.25	0.25
	6	0.273	0.271	0.27	0.271	0.274	0.278	0.284	0.292	0.302
	7	0.292	0.292	0.294	0.299	0.304	0.312	0.323	0.338	0.359
	8	0.308	0.319	0.328	0.337	0.346	0.357	0.371	0.39	0.418
	9	0.321	0.362	0.382	0.395	0.406	0.417	0.429	0.445	0.472
	10	0	0.5	0.5	0.5	0.5	0.5	0.5	0.5	0.5

(b)

Fig. 11 Dependence of the state probability s_1 of MICSA, k = m = 2, and O = 2, upon the error probabilities of the CUT(1).
(a) Graphic representation. (b) Matrix representation.

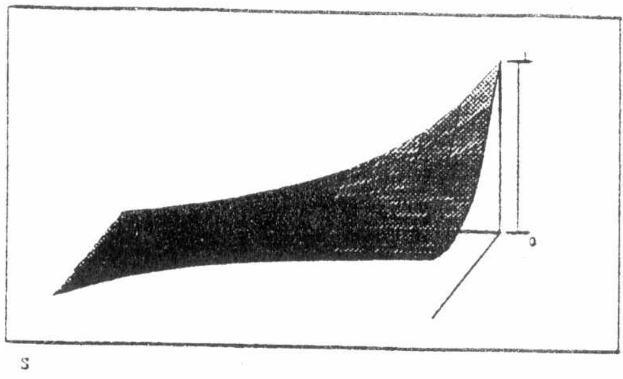

(a)

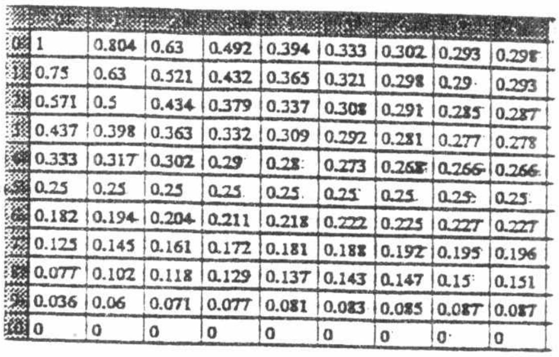

0	1	0.804	0.63	0.492	0.394	0.333	0.302	0.293	0.298
1	0.75	0.63	0.521	0.432	0.365	0.321	0.298	0.29	0.293
2	0.571	0.5	0.434	0.379	0.337	0.308	0.291	0.285	0.287
3	0.437	0.398	0.363	0.332	0.309	0.292	0.281	0.277	0.278
4	0.333	0.317	0.302	0.29	0.28	0.273	0.268	0.266	0.266
S = 5	0.25	0.25	0.25	0.25	0.25	0.25	0.25	0.25	0.25
6	0.182	0.194	0.204	0.211	0.218	0.222	0.225	0.227	0.227
7	0.125	0.145	0.161	0.172	0.181	0.188	0.192	0.195	0.196
8	0.077	0.102	0.118	0.129	0.137	0.143	0.147	0.15	0.151
9	0.036	0.06	0.071	0.077	0.081	0.083	0.085	0.087	0.087
10	0	0	0	0	0	0	0	0	0

(b)

Fig.12 Dependence of the state probability s_2 of MICSA, k = m = 2, and O = 2, upon the error probabilities of the CUT(1). (a) Graphic representation. (b) Matrix representation.

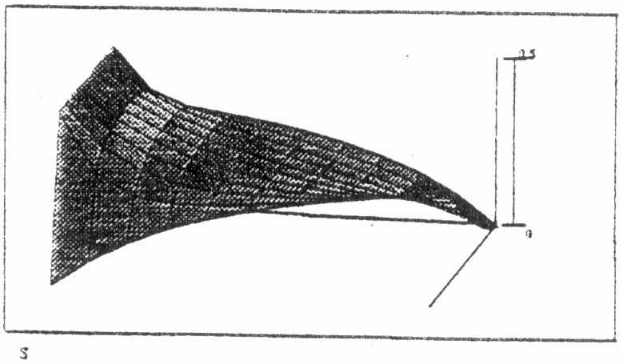

(a)

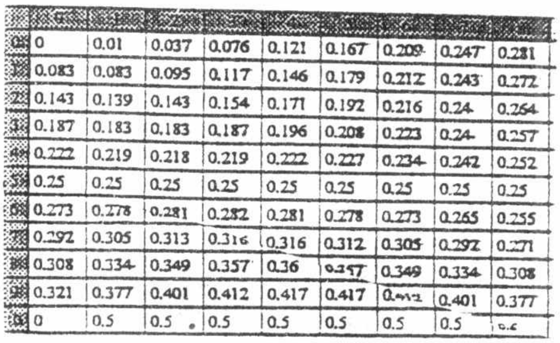

0	0	0.01	0.037	0.076	0.121	0.167	0.209	0.247	0.281
1	0.083	0.083	0.095	0.117	0.146	0.179	0.212	0.243	0.272
2	0.143	0.139	0.143	0.154	0.171	0.192	0.216	0.24	0.264
3	0.187	0.183	0.183	0.187	0.196	0.208	0.223	0.24	0.257
4	0.222	0.219	0.218	0.219	0.222	0.227	0.234	0.242	0.252
S = 5	0.25	0.25	0.25	0.25	0.25	0.25	0.25	0.25	0.25
6	0.273	0.278	0.281	0.282	0.281	0.278	0.273	0.265	0.255
7	0.292	0.305	0.313	0.316	0.316	0.312	0.305	0.292	0.271
8	0.308	0.334	0.349	0.357	0.36	0.357	0.349	0.334	0.308
9	0.321	0.377	0.401	0.412	0.417	0.417	0.412	0.401	0.377
10	0	0.5	0.5	0.5	0.5	0.5	0.5	0.5	0.5

(b)

Fig. 13 Dependence of the state probability s_3 of MICSA, k = m = 2, and O = 2, upon the error probabilities of the CUT(1). (a) Graphic representation. (b) Matrix representation.

3.2 Structure of MICSA, k = 2, m = 1, Outputs (O) = 2, CUT(2) :

Fig. 14 is composed of 2-stages (k), NPP-MISR, the CUT(2) has one input and two outputs. The last outputs of the 2-stage MISR are connecting to the input of the CUT (2), while the outputs of the CUT(2) are fedback to the first and second stages of MISR through XOR circuits. Fig. 15 represents the MSD for Fig. 14, and its TPM is shown in Fig. 16.

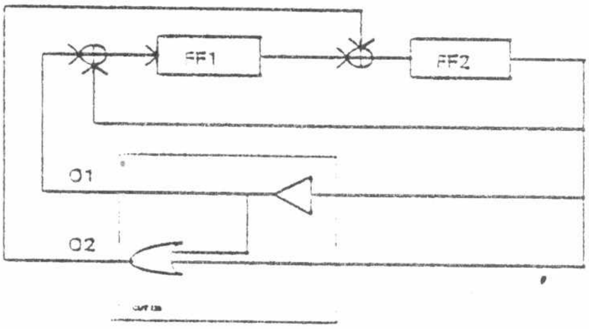

Fig. 14 Structure for MICSA, with k = 2, m = 1, O = 2, CUT(2).

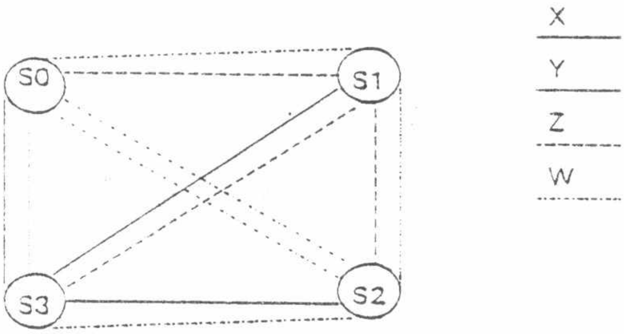

Fig. 15 MSD for MICSA, with k = 2, m = 1, O = 2, CUT(2).

$$
M2 = \begin{array}{c|cccc}
 & s_0 & s_1 & s_2 & s_3 \\
\hline
s_0 & Y & Z & W & X \\
s_1 & W & X & Y & Z \\
s_2 & W & Z & Y & X \\
s_3 & Y & X & W & Z
\end{array}
$$

Fig. 16 TPM for MICSA, with k = 2, m = 1, O = 2, CUT(2).

From Fig. 16 the local balance equations are calculated as :

$$
\begin{aligned}
(1-Y)s_0 &= Ws_1 + Ws_2 + Ys_3 \\
(1-X)s_1 &= Zs_0 + Zs_2 + Xs_3 \\
(1-Y)s_2 &= Ws_0 + Ys_1 + Ws_3 \\
s_0 + s_1 + s_2 + s_3 &= 1
\end{aligned}
\qquad (18)
$$

The equations (18) are solved using [16]; giving :

$$
\left.
\begin{aligned}
s_0 &= \frac{-(ZW^2 + XW + W^2 - XW^2 + Y - XY - Y^2 + XY^2 - Y^{2)}}{(-1 + Y - W)} \\
s_1 &= YZ - XY + X + ZW - XW \\
s_2 &= \frac{(-W + XW - XY + XY^2 + ZW^2 - Y^2Z - XW^2)}{(-1 + Y - W)} \\
s_3 &= -Y - YZ + XY + 1 - X - W - ZW + XW
\end{aligned}
\right\} \qquad (19)
$$

Substituting the values of X, Y, Z, and W in equation (19) by the corresponding values of p, q as described in Table (1), and simplifying the results, we get :

$$s_0 = \frac{(-1+p)(-1-2pq^2-4p^2q+4p^2q^2+pq+q+p^2)}{(2-2q+2pq-p)} \qquad (20)$$

$$s_1 = -pq + p - p^2 + 2p^2q \qquad (21)$$

$$s_2 = \frac{-(-1+p)(1-2pq^2-p-4p^2q+4p^2q^2+3pq-q+p^2)}{(2-2q+2pq-p)} \qquad (22)$$

$$s_3 = pq + p^2 - 2p^2q \qquad (23)$$

Equations (20 - 23) are plotted in Figures (17 - 20) each figure is followed by a matrix giving the values of the state probability against the error probability p and q.

These figures show that the state probability is depending on the error probability of the CUT(2), the threshold value (1/4) which is the SS-AEP of MISR in the open loop is greater or less than the probability of the corresponding CSA with MISR in closed loop system, but they are equal for the equally likely error model when p = q = 0.5, which is the same as the one given by [6].

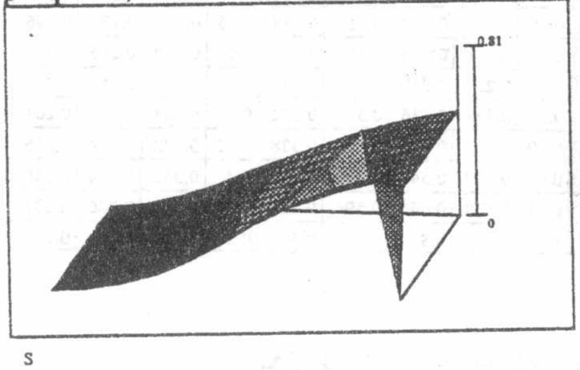

(a)

S =

	0	1	2	3	4	5	6	7	8
0	0.5	0.5	0.5	0.5	0.5	0.5	0.5	0.5	0.5
1	0.469	0.463	0.458	0.454	0.451	0.45	0.452	0.459	0.478
2	0.427	0.419	0.412	0.406	0.402	0.4	0.402	0.411	0.433
3	0.375	0.367	0.361	0.355	0.351	0.35	0.352	0.359	0.376
4	0.315	0.31	0.306	0.303	0.301	0.3	0.301	0.305	0.313
5	0.25	0.25	0.25	0.25	0.25	0.25	0.25	0.25	0.25
6	0.183	0.188	0.193	0.197	0.199	0.2	0.199	0.195	0.189
7	0.118	0.128	0.137	0.144	0.148	0.15	0.148	0.142	0.132
8	0.06	0.074	0.085	0.093	0.098	0.1	0.098	0.092	0.08
9	0.017	0.029	0.038	0.044	0.049	0.05	0.049	0.044	0.036
10	0	0	0	0	0	0	0	0	0

(b)

Fig. 17 Dependence of the state probability s_0 of MICSA, with NPP, k =2, m = 1, and O = 2 upon the error probabilities of the CUT(2). (a) Graphic representation. (b) Matrix representation.

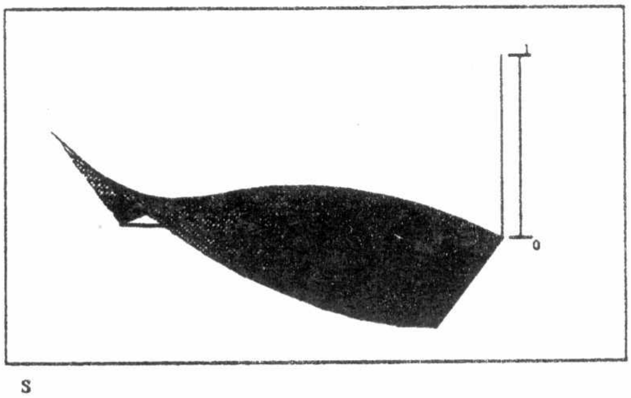

S =

	0	1	2	3	4	5	6	7	8
0	0	0	0	0	0	0	0	0	0
1	0.09	0.082	0.074	0.066	0.058	0.05	0.042	0.034	0.026
2	0.16	0.148	0.136	0.124	0.112	0.1	0.088	0.076	0.064
3	0.21	0.198	0.186	0.174	0.162	0.15	0.138	0.126	0.114
4	0.24	0.232	0.224	0.216	0.208	0.2	0.192	0.184	0.176
5	0.25	0.25	0.25	0.25	0.25	0.25	0.25	0.25	0.25
6	0.24	0.252	0.264	0.276	0.288	0.3	0.312	0.324	0.336
7	0.21	0.238	0.266	0.294	0.322	0.35	0.378	0.406	0.434
8	0.16	0.208	0.256	0.304	0.352	0.4	0.448	0.496	0.544
9	0.09	0.162	0.234	0.306	0.378	0.45	0.522	0.594	0.666
10	0	0.1	0.2	0.3	0.4	0.5	0.6	0.7	0.8

(a) (b)

Fig. 18 Dependence of the state probability s_1 of MICSA, $k = 2$, $m = 1$, and $O = 2$ upon the error probabilities of the CUT (2).
(a) Graphic representation. (b) Matrix representation.

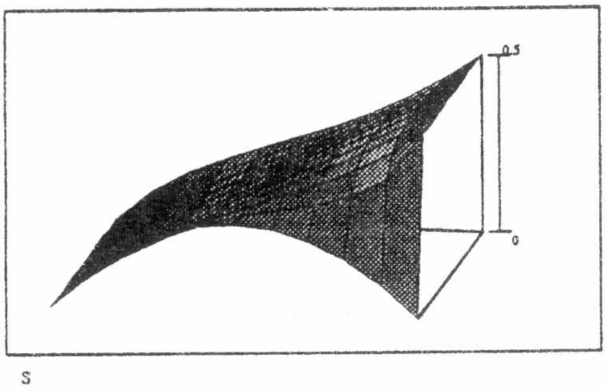

S =

	0	1	2	3	4	5	6	7	8
0	0.5	0.5	0.5	0.5	0.5	0.5	0.5	0.5	0.5
1	0.431	0.437	0.442	0.446	0.449	0.45	0.448	0.441	0.422
2	0.373	0.381	0.388	0.394	0.398	0.4	0.398	0.389	0.367
3	0.325	0.333	0.339	0.345	0.349	0.35	0.348	0.341	0.324
4	0.285	0.29	0.294	0.297	0.299	0.3	0.299	0.295	0.287
5	0.25	0.25	0.25	0.25	0.25	0.25	0.25	0.25	0.25
6	0.217	0.212	0.207	0.203	0.201	0.2	0.201	0.205	0.211
7	0.182	0.172	0.163	0.156	0.152	0.15	0.152	0.158	0.168
8	0.14	0.126	0.115	0.107	0.102	0.1	0.102	0.108	0.12
9	0.083	0.071	0.062	0.056	0.051	0.05	0.051	0.056	0.064
10	0	0	0	0	0	0	0	0	0

(a) (b)

Fig. 19 Dependence of the state probability s_2 of MICSA, $k = 2$, $m = 1$, and $O = 2$ upon the error probabilities of the CUT(2).
(a) Graphic representation. (b) Matrix representation.

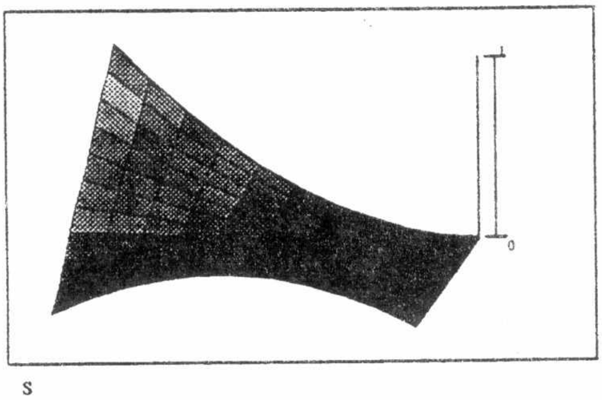

S =

	0	1	2	3	4	5	6	7	8
0	0	0	0	0	0	0	0	0	0
1	0.01	0.018	0.026	0.034	0.042	0.05	0.058	0.066	0.074
2	0.04	0.052	0.064	0.076	0.088	0.1	0.112	0.124	0.136
3	0.09	0.102	0.114	0.126	0.138	0.15	0.162	0.174	0.186
4	0.16	0.168	0.176	0.184	0.192	0.2	0.208	0.216	0.224
5	0.25	0.25	0.25	0.25	0.25	0.25	0.25	0.25	0.25
6	0.36	0.348	0.336	0.324	0.312	0.3	0.288	0.276	0.264
7	0.49	0.462	0.434	0.406	0.378	0.35	0.322	0.294	0.266
8	0.64	0.592	0.544	0.496	0.448	0.4	0.352	0.304	0.256
9	0.81	0.738	0.666	0.594	0.522	0.45	0.378	0.306	0.234
10	1	0.9	0.8	0.7	0.6	0.5	0.4	0.3	0.2

(a) (b)

Fig. 20 Dependence of the state probability s_3 of MICSA, $k = 2$, $m = 1$, and $O = 2$ upon the error probabilities of the CUT(2).
(a) Graphic representation. (b) Matrix representation.

4. The Improved Multiple Inputs Compact Signature Analysis (IMICSA) :

In the following sections different cases studies of the Improved Multiple Inputs Compact Signature Analysis (IMICSA), in which the k^{th} stage of the MISR (PP and NPP) is not connected to any of the CUT's inputs are introduce. This group of cases is used to validate the derived theorem.

4.1 Structure of IMICSA, PP, k = 4, m = 3, CUT(3) :

Fig. 21 is composed of 4-stages PP-LFSR, three outputs - not any of them is the last stage output - are connected to the CUT(3) inputs, and the outputs of the CUT(3) is fedback to the inputs of the of MISR through XOR circuits. Fig. 22 represents the MSD for Fig. 21, and its TPM is shown in Fig. 23.

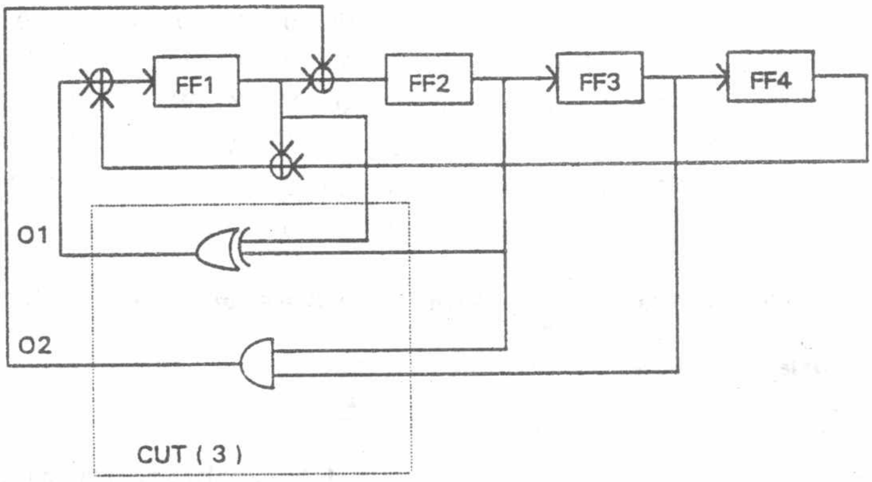

Fig. 21 IMICSA, PP, k = 4, m = 3, O = 2, CUT(3).

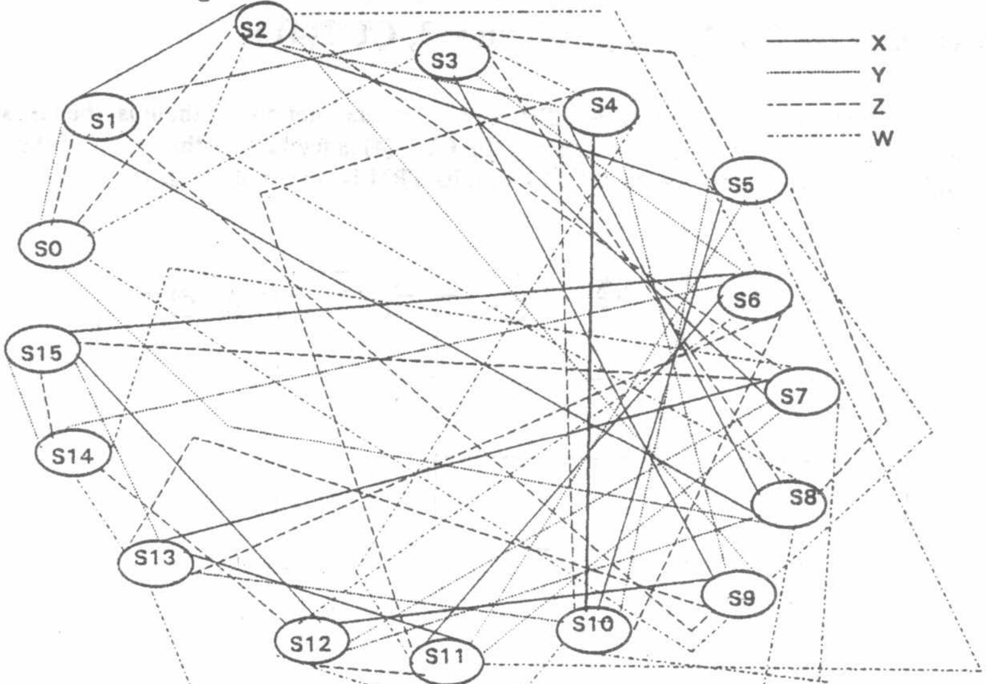

Fig. 22 MSD for IMICSA , PP, k = 4, m = 3, O = 2, CUT (3).

$$M3 = \begin{array}{c|cccccccccccccccc} & s_0 & s_1 & s_2 & s_3 & s_4 & s_5 & s_6 & s_7 & s_8 & s_9 & s_{10} & s_{11} & s_{12} & s_{13} & s_{14} & s_{15} \\ \hline s_0 & X & Y & Z & W & 0 & 0 & 0 & 0 & 0 & 0 & 0 & 0 & 0 & 0 & 0 & 0 \\ s_1 & Z & W & X & Y & 0 & 0 & 0 & 0 & 0 & 0 & 0 & 0 & 0 & 0 & 0 & 0 \\ s_2 & 0 & 0 & 0 & 0 & Y & X & W & Z & 0 & 0 & 0 & 0 & 0 & 0 & 0 & 0 \\ s_3 & 0 & 0 & 0 & 0 & W & Z & Y & X & 0 & 0 & 0 & 0 & 0 & 0 & 0 & 0 \\ s_4 & 0 & 0 & 0 & 0 & 0 & 0 & 0 & 0 & X & Y & Z & W & 0 & 0 & 0 & 0 \\ s_5 & 0 & 0 & 0 & 0 & 0 & 0 & 0 & 0 & Z & W & X & Y & 0 & 0 & 0 & 0 \\ s_6 & 0 & 0 & 0 & 0 & 0 & 0 & 0 & 0 & 0 & 0 & 0 & 0 & W & Z & Y & X \\ s_7 & 0 & 0 & 0 & 0 & 0 & 0 & 0 & 0 & 0 & 0 & 0 & 0 & Y & X & W & Z \\ s_8 & Y & X & W & Z & 0 & 0 & 0 & 0 & 0 & 0 & 0 & 0 & 0 & 0 & 0 & 0 \\ s_9 & W & Z & Y & X & 0 & 0 & 0 & 0 & 0 & 0 & 0 & 0 & 0 & 0 & 0 & 0 \\ s_{10} & 0 & 0 & 0 & 0 & X & Y & Z & W & 0 & 0 & 0 & 0 & 0 & 0 & 0 & 0 \\ s_{11} & 0 & 0 & 0 & 0 & Z & W & X & Y & 0 & 0 & 0 & 0 & 0 & 0 & 0 & 0 \\ s_{12} & 0 & 0 & 0 & 0 & 0 & 0 & 0 & 0 & Y & X & W & Z & 0 & 0 & 0 & 0 \\ s_{13} & 0 & 0 & 0 & 0 & 0 & 0 & 0 & 0 & W & Z & Y & X & 0 & 0 & 0 & 0 \\ s_{14} & 0 & 0 & 0 & 0 & 0 & 0 & 0 & 0 & 0 & 0 & 0 & 0 & Z & W & X & Y \\ s_{15} & 0 & 0 & 0 & 0 & 0 & 0 & 0 & 0 & 0 & 0 & 0 & 0 & X & Y & Z & W \end{array}$$

Fig. 23 TPM for IMICSA with k > m (k = 4, m = 3), O = 2, CUT (3).

Matrix M3 is a double stochastic matrix, which means that :

$$S_0 = S_1 = S_2 = \ldots\ldots\ldots\ldots\ldots = S_{15} = \frac{1}{16}$$

This shows that the threshold for 1/16 which is the SS-AEP of the open loop is equal to the probability of existing of all statesof CSA with MISR when last stage is not connected to any of the CUT's inputs.

4.2 Structure of IMICSA, NPP, k = 4, m = 3, CUT(4) :

Fig. 24 is composed of 4-stages NPP-MISR, three outputs - not any of them is the last stage output - are connected to the CUT(4) inputs, and the outputs of the CUT (4) is fedback to the inputs of the of MISR through XOR circuits. Fig. 25 represents the MSD for Fig. 24, and its TPM is shown in Fig. 26.

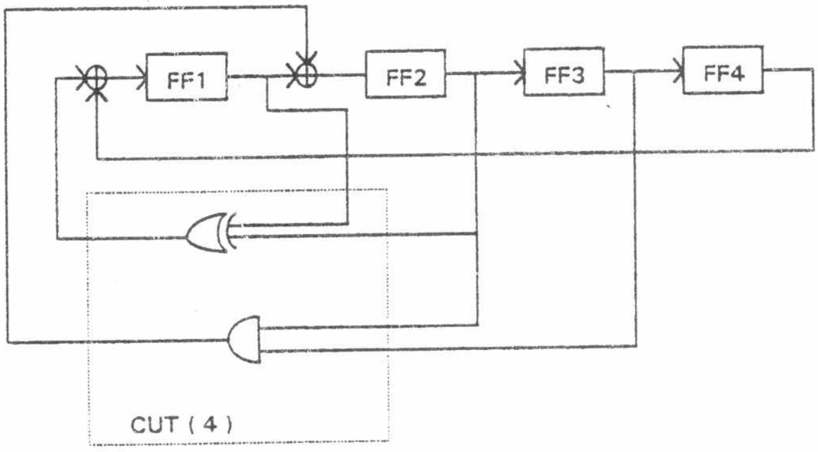

Fig. 24 IMICSA, NPP, k = 4, m = 2, O = 2, O = 2, CUT(4).

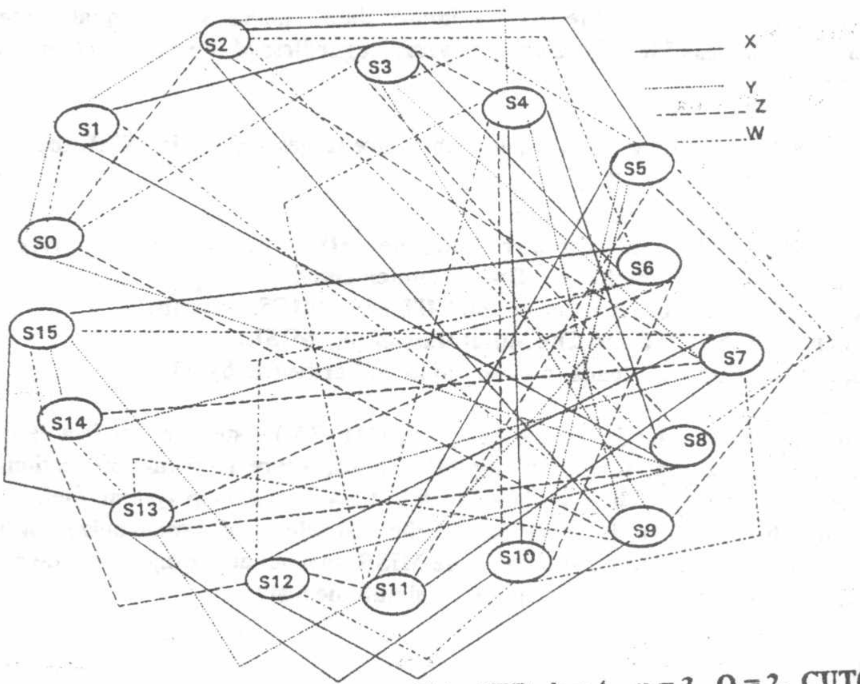

Fig. 25 MSD for IMICSA, NPP, k = 4, m = 3, O = 2, CUT(4).

$$M4 = \begin{array}{c|cccccccccccccccc}
 & s_0 & s_1 & s_2 & s_3 & s_4 & s_5 & s_6 & s_7 & s_8 & s_9 & s_{10} & s_{11} & s_{12} & s_{13} & s_{14} & s_{15} \\
s_0 & X & Y & Z & W & 0 & 0 & 0 & 0 & 0 & 0 & 0 & 0 & 0 & 0 & 0 & 0 \\
s_1 & W & Z & Y & X & 0 & 0 & 0 & 0 & 0 & 0 & 0 & 0 & 0 & 0 & 0 & 0 \\
s_2 & 0 & 0 & 0 & 0 & Y & X & W & Z & 0 & 0 & 0 & 0 & 0 & 0 & 0 & 0 \\
s_3 & 0 & 0 & 0 & 0 & Z & W & X & Y & 0 & 0 & 0 & 0 & 0 & 0 & 0 & 0 \\
s_4 & 0 & 0 & 0 & 0 & 0 & 0 & 0 & 0 & X & Y & Z & W & 0 & 0 & 0 & 0 \\
s_5 & 0 & 0 & 0 & 0 & 0 & 0 & 0 & 0 & W & Z & Y & X & 0 & 0 & 0 & 0 \\
s_6 & 0 & 0 & 0 & 0 & 0 & 0 & 0 & 0 & 0 & 0 & 0 & 0 & W & Z & Y & X \\
s_7 & 0 & 0 & 0 & 0 & 0 & 0 & 0 & 0 & 0 & 0 & 0 & 0 & X & Y & Z & W \\
s_8 & Y & X & W & Z & 0 & 0 & 0 & 0 & 0 & 0 & 0 & 0 & 0 & 0 & 0 & 0 \\
s_9 & Z & W & X & Y & 0 & 0 & 0 & 0 & 0 & 0 & 0 & 0 & 0 & 0 & 0 & 0 \\
s_{10} & 0 & 0 & 0 & 0 & X & Y & Z & W & 0 & 0 & 0 & 0 & 0 & 0 & 0 & 0 \\
s_{11} & 0 & 0 & 0 & 0 & W & Z & Y & X & 0 & 0 & 0 & 0 & 0 & 0 & 0 & 0 \\
s_{12} & 0 & 0 & 0 & 0 & 0 & 0 & 0 & 0 & Y & X & W & Z & 0 & 0 & 0 & 0 \\
s_{13} & 0 & 0 & 0 & 0 & 0 & 0 & 0 & 0 & Z & W & X & Y & 0 & 0 & 0 & 0 \\
s_{14} & 0 & 0 & 0 & 0 & 0 & 0 & 0 & 0 & 0 & 0 & 0 & 0 & Z & W & X & Y \\
s_{15} & 0 & 0 & 0 & 0 & 0 & 0 & 0 & 0 & 0 & 0 & 0 & 0 & Y & X & W & Z
\end{array}$$

Fig. 26 TPM for IMICSA with k > m (k = 4, m = 3), O = 2, CUT (4).

Matrix M4 is a double stochastic matrix, which means that :

$$S_0 = S_1 = S_2 = \ldots\ldots\ldots\ldots\ldots = S_{15} = \frac{1}{16}$$

This shows that the threshold for 1/16 which is the SS-AEP of the open loop is equal to the probability of existing of all states of CSA with MISR when last stage is not connected to any of the CUT's inputs.

5. Conclusions :

1- The SS-AEP of MICSA for k = m, and for k > m with the k^{th} stage connected to one of the CUT inputs is not necessarily the conventional 2^{-k} limit (k being the number of stages of the signature analyzer). Instead, it is shown that any value from 0 to 1 is attainable as a final value of SS-AEP, depending on : the structure of the CUT, and the construction of the MICSA. These factors, on which SS-AEP of MICSA depends, make its use as a digital circuit test system impractical.

2- The hardware condition for SS-AEP of MICSA, to be equal $/2^k$ is deduced. This has led to what we called the Improved Multiple Input Compact Signature Analysis (IMICSA). The results are mathematically proved and formulated to the theorem which dictates that : " For the CSA which is constructed from MISR, if

its k^{th} stage is not connected to any of the CUT's inputs, then, The SS-AEP is equal to the reciprocal of 2^k, where k is the number of the stages of the signature analyzer, regardless of the construction of CUT, or the initial state of signature analyzer. "

For the IMICSA it is found that :

A) The steady state AEP is a function of k , and the more stages you use in MISR the better is the steady state AEP, (SS-AEP equal 2^{-k}).

B) SS-AEP is shown to be independent of :

- **The type of the polynomial used in realizing the MISR (primitive or non primitive).**
- **The particular way by which the MISR is implemented.**
- **The location of points for connecting the CUT with MICSA circuit.**
- **The structure of the CUT and The initial state of the MISR.**

C) In addition, the IMICSA still leads to a reduction of hardware by 50%.

3-These results introduce

the Improved Multiple Input Compact Signature Analysis (IMICSA) system, which is a new discipline in digital system testing, it provides functional testing of digital systems, where all of the interactions of timing, loading, temperature, and noise come to play. The use of feedback in CSA closed loop system makes the system response insensitive to external disturbances. It overcomes the problem of synchronization between test pattern generator and test response compression technique. The MISR have an advantage over the single input signature analyzer that it can test several test points or several units simultaneously.

REFERENCES

[1] R. Howard, " Dynamic Probabilistic System, Markov Models" J. Wiley & Sons, Inc., 1971.

[2] R. A. Frohwerk, " Signature analysis : A New Digital Field Services Method," Hewlett -Packard J., pp. 2-8, May 1977.

[3] A. Cstover ," Automatic Test Equipment ", MC Graw-Hill inc. 1984.

[4] A. Miczo, " Digital Logic Testing and Simulation", Harper & Row, Inc.1984.

[5] P. H. Bardell, W. H. Mc Anney, and J. Savir " Built-in Test for VLSI: Pseudo Random Techniques" New York: J. Wiley & Sons, 1987.

[6] T. W. Williams, W. Daehn, M. Gruetzner," Bounds and Analysis of Aliasing Error in LFSR," IEEE Trans. on Computer-Aided Design, vol. 7, pp. 75-83.1988.

[7] Williams T. W., and Daehn, W., " Aliasing Errors in Multiple Input Signature Analysis Registers" IEEE Int. Conf. on Comp. Aided Design, pp 338-345, April 1989.

[8] Olivo, P., Damiani, M., and Ricco, B. " On the Design of Multiple Input Shift Register for Analysis Testing " IEEE Int. Test Conf., pp 936, 1989.

[9] S. Ercolani, M. Favalli, M. Damiani, and B. Ricco " Improved Testability Evaluation in Combination Logic Network " in Proc. of IEEE Int. Conf. On Computer Design, pp. 352 - 355, 1989.

[10] M. Abramovici, M. A. Breuer, A. D. Friedman," Digital System Testing and Testable Design ", AT&T Bell Laboratories and W. H. Freeman and Company , 1990.

[11] M. Damiani, P. Olivo, M. Favalli, and B. Ricco " Aliasing in Signature Analysis Testing with Multiple- Input Shift-Register" , IEEE Transaction on CAD, Vol. 12, pp. 1344 - 1353, 1990.

[12] Francis C. Wang, " Digital Circuit Testing "Academic Press, Inc. San Diego, California 92101. 1991.

[13] France C. Wang ," Digital Circuit Testing : A Guide to DFT and Other Techniques", 1991 by ACADEMIC PRESS, INC.

[14] M. El Moatasem, A. Seddik," PC- Based signature Analysis: An Optimization Technique for Fault Detection in Digital Electronic Systems," Inter. Special Conf. on Multiple Criteria Decision Making (MCDM) , M.T.C., Cairo, Egypt. 3-5 March 1992.

[15] A. Seddik ," Microcomputer Based Automatic Testing System Through Signature Analysis", M. Sc Degree. M.T.C , Cairo, 1992.

[16] Mathsoft " MATHCAD 5.0 " © 1994 Mathsoft Inc. Version5.0 International Correct Spell © 1993 by Houghton Company.

[17] M. S. Ghoniemy, A. seddik," Automatic Testing of Digital Circuits Through Signature Analysis," IASTED Inter. Conf. on Modeling and Simulation, Pittsburgh, Pennsylvnia , USA. May 2-4 , 1994.

[18] R. H. Seireg M.S.Ghoniemy, S.F.Bahgat,A.Seddik, "Compact Signature Analysis " National Conf. for Radio, Feb. 1995.

[19] M . S. Ghoniemy, R. H. Seireg, S. F. Bahgat, A. Seddik," Improving the Performance of Compact Signature Analysis Using LFSR." 13'th National Radio Science Conf. , Cairo, Egypt. 19-21 March 1996.